

Novel Soft Switching Inverter for Brushless DC Motor using Fuzzy Logic

N. Muruganantham¹ and S. Palani²

¹*Asst. Professor of Electrical & Electronics Engineering,*

Periyar Maniammai University, Periyar Nagar,

Vallam-613 403, Thanjavur (dt.), Tamil Nadu, India

E-mail: murugaksr@rediffmail.com

²*Dean of Electronics Engineering, Sudharsan Engineering College,*

Sathyamangalam-622501, Pudukkottai (dt.), Tamil Nadu, India

E-mail: keeranur_palani@yahoo.co.in

Abstract

Brushless DC motor (BLDCM) has been broadly used in drive systems and servo control because of its fast response, high power density, high efficiency, low inertia, high reliability and maintenance free. It is however driven by a hard-switching PWM inverter, which has low switching frequency, high switching loss, high electro-magnetic interference (EMI), high acoustic noise and low efficiency, etc. To solve these problems of the hard switching inverter, many soft switching inverters have been designed in the past. Unfortunately, high device voltage stress, large dc link voltage ripples, complex control scheme and so on are noticed in the soft switching inverters. This paper introduces a novel fuzzy logic based soft-switching inverter using transformer, which can generate dc link voltage notches during chopping which minimize the drawbacks of soft switching. Hence all switches work in zero voltage switching condition. The operation principle and control scheme of the inverter are analyzed and performance of the fuzzy controller is compared with conventional PI controller. The simulation results show that the fuzzy controller renders a better transient response than the PI controller resulting in negligible overshoot and smaller settling time. Simulation results are proposed to verify the theoretical analysis.

Keywords: Brushless DC Motor, Fuzzy Logic Controller, Zero-Voltage Switching, Zero-Current Switching.

Introduction

The operating characteristics of brushless dc motor resemble that of a conventional commutated dc permanent magnet motor but without the mechanical commutators and brushes. Hence many problems associated with brushes such as radio-frequency interference and sparking which is the potential source of ignition inflammable atmosphere are eliminated. It is usually supplied by a hard switching pulse width modulation (PWM) inverter, which normally has relatively low efficiency since the power losses across the switching devices are high. The high dv/dt and di/dt will result in severe electromagnetic interference (EMI) and rigorous problems with the reverse recovery of the freewheeling diodes, especially in high switching frequency. As the switching frequency of the hard switching is not very high when the switching frequency is within audio spectrum, it may produce severe acoustic noise. Furthermore, there is “turning off current spike” for inductive load or “turning on voltage spike” for capacitive load with a hard switching inverter, which can produce excessive localized hot spots and damage power semiconductor switches. In order to solve these problems, many soft switching inverters have been designed.

Soft switching operation of the power inverter has attracted much attention in the recent decades. In electric motor drive applications, soft switching inverters are usually classified into three categories, namely, resonant pole inverter, resonant dc link inverter and resonant ac link inverter [1]. Resonant ac link inverter is not suitable to BLDC motor drivers. Resonant dc link inverter [2], [3] has disadvantages such as high voltage stress of the switches, high dc link voltage ripple and large resonant inductor power losses. It is with discrete pulse modulation (DPM) control that it is hard to achieve real PWM control and will result in sub-harmonics. Several quasi-parallel resonant dc link inverters were designed to solve these problems, but these inverters require an additional main conduction path switch, which will increase the conduction power losses of the inverter [4], [5]. The another problem associated with the resonant dc link is that whichever phase is needed to commutate, the dc link voltage of that phase is reduced to zero temporarily, which will affect the operation of other phases.

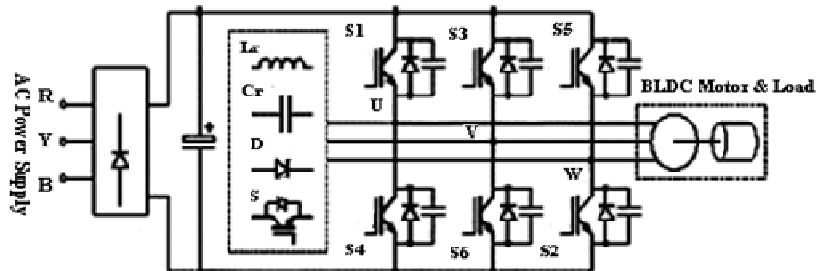


Figure 1: Soft switching inverter topology.

The structure of the soft switching inverter topology [6]–[11] is shown in Fig. 1. Each pole comprises a resonant inductor and a pair of resonant capacitors at each

phase leg. These capacitors are directly connected in parallel to the main inverter switches in order to achieve zero-voltage switching (ZVS) condition. In contrast to the resonant dc link inverter, the dc link voltage remains unaffected during the resonant transitions. The resonant transitions occur separately at each resonant pole when the corresponding main inverter switch needs switching. Therefore the main switches in the inverter phase legs can switch independently from each other and choose the commutation period without restraint. Moreover, there is no additional main conduction path switch. Thus, the normal operation of the soft switching inverter is entirely the same as that of conventional hard switching inverter.

The auxiliary resonant commutated pole (ARCP) inverter [6] and the ordinary resonant snubber inverter [7] provide a ZVS condition without increasing the device voltage and current stress. These inverters are able to achieve real PWM control. However, they require a stiff dc link capacitor bank that is center-tapped to accomplish commutation. The center voltage of dc link is susceptible to drift that may affect the operation of the resonant circuit. The resonant transition inverter [8], [9] only uses one auxiliary switch, whose switching frequency is much higher than that obtained using the main switches. Thus, it will limit the switching frequency of the inverter. A Y-configured resonant snubber inverter [10] has a floating neutral voltage that may cause overvoltage failure of the auxiliary switches. A delta configured resonant snubber inverter [11] avoids the floating neutral voltage and is suitable for multiphase operation without circulating currents between the off-state branch and its corresponding output load. However, the inverter requires three inductors and six auxiliary switches. Hence the inverter cost gets increased and in addition occupies larger space.

Soft switching inverters have been used in induction motor drive applications. They are usually required to change two phase switching states simultaneously to obtain a resonant path. It is not suitable for BLDC motor drive system as only one switch is needed to change the switching state in a PWM cycle. The resonant pole inverter [12] provides low switching power losses, low inductor power losses, low switching noise and simple control scheme. However, the conventional PI controller is used in the speed control. Hence the transient response of the motor is significantly affected. Also, PI controller's tuning requires the mathematical model of the plant being controlled. The design of fuzzy controller doesn't require any mathematical model of the plant. It gives good transient characteristics to the system. This is the motivation to apply a fuzzy controller to speed control of a BLDC motor drive. In this paper, a new fuzzy logic based Soft switching inverter is designed for BLDC motor drive systems which is easy to implement in industries. PI controller has also been implemented for comparison with the proposed fuzzy based control scheme.

Soft switching Inverter Topology

A distinctive controller for BLDC motor drive system [13] is shown in Fig. 2. The rotor position is sensed by a hall effect sensor or a slotted optical disk, providing three square waves with phase shift of 120° . These signals are decoded by a combinatorial logic to provide the firing signals for 120° conduction on each of the three phases. The

simulation diagram of fuzzy based Soft switching inverter for BLDC motor drive system is shown in Fig. 3. The system contains a diode bridge rectifier, a resonant circuit, a conventional 3Φ inverter and control circuitry. The resonant circuit consists of three auxiliary switches (S_a , S_b , S_c), one transformer with turns ratio 1 : n, and two diodes D_{fp} , D_r .

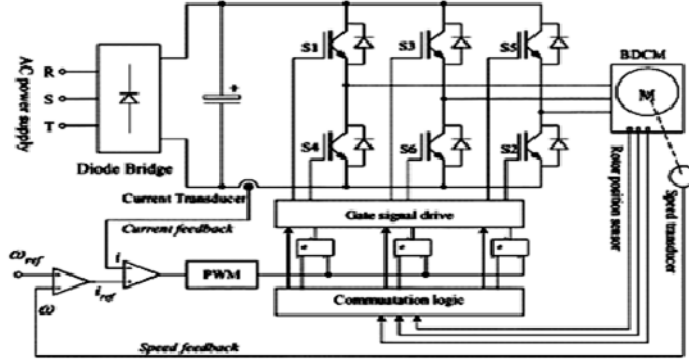


Figure 2: Distinctive controller for BLDC motor drive system.

Diode D_{fp} is connected in parallel to the primary winding of the transformer and diode D_r is serially connected with secondary winding across the dc link. There is one snubber capacitor connected in parallel to each switch of phase leg. The snubber capacitor resonates with the primary winding of the transformer. The emitters of the three auxiliary switches are connected together. Thus, the gate drive of these auxiliary switches can use one common output dc power supply.

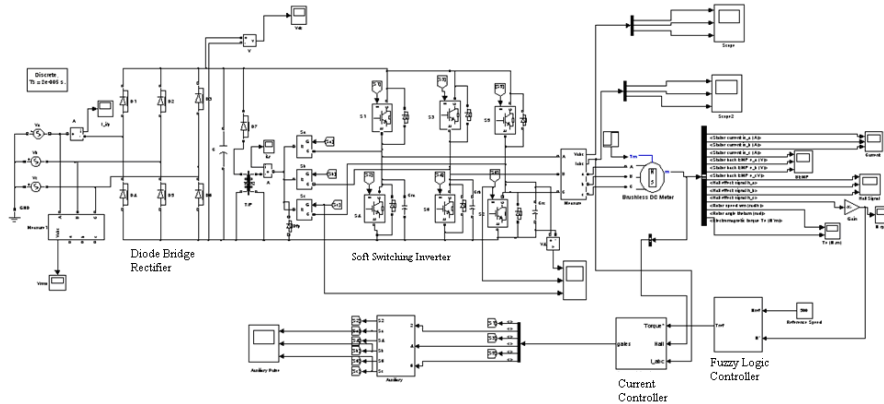


Figure 3: Simulation diagram of fuzzy based Soft switching inverter for BLDC motor drive system

In an entire PWM cycle, all the six main switches can be turned off in the ZVS condition as the snubber capacitors (C_{ra} , C_{rb} , C_{rc}) can slow down the voltage rise rate.

This enables the turn-off power losses be reduced and the turn-off voltage spike eliminated. Before turning on the main switches, the corresponding auxiliary switch (S_a , S_b , S_c) must be turned on ahead. The snubber capacitor discharges and the main switches get the ZVS condition. The equivalent circuit of Soft switching inverter is shown in Fig. 4, where V_s is the dc link voltage, i_{Lr} is the transformer primary winding current, u_{S6} is the voltage drop across the switch S_6 (i.e., snubber capacitor C_{rb} voltage), and I_o is the load current. The waveforms of the switches (S_6 , S_b) gate signal, PWM signal, main switch S_6 voltage drop (u_{S6}), and the transformer primary winding current (i_{Lr}) are shown in Fig. 5. In Fig. 5, the time interval ($t_0 - t_6$) is divided into seven switching modes from which commutation instant of main and auxiliary switches can be clearly known.

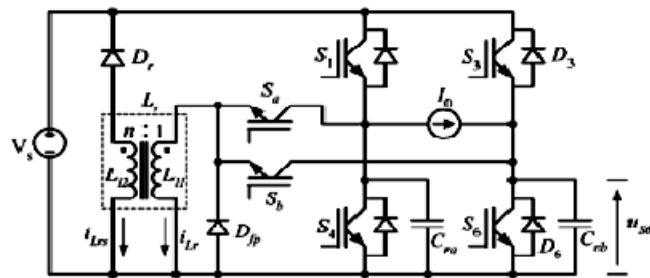


Figure 4: Equivalent circuit of Soft switching inverter.

During phase current commutation, the switching state is changed from one lower switch to another lower switch (e.g., turn off S_6 and turn on S_2), S_6 is turned off directly in ZVS condition and turning on auxiliary switch S_c . Now the snubber capacitor C_{rc} discharges its charged voltage through Switch S_c and the switch S_2 is in ZVS condition

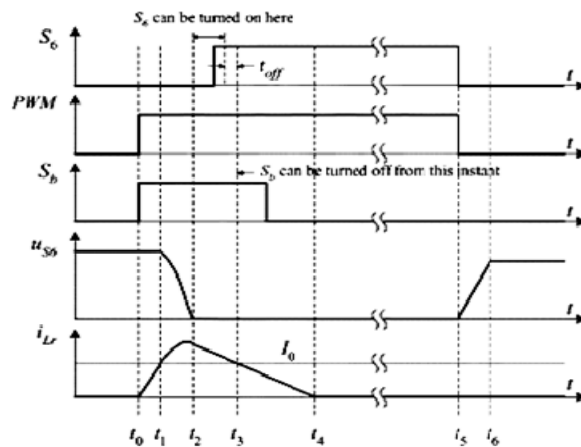


Figure 5: Waveforms of the equivalent circuit.

Design Considerations

The design considerations are summarized as follows with the assumption that the inductance of BLDC motor is much higher than the transformer leakage inductance.

- Determine the value of snubber capacitance C_r and the parameters of transformer;
- Select the main and auxiliary switches;
- Design the control circuitry for the main and auxiliary switches.

The turns ratio (1 : n) of the transformer is determined ahead. From [12] “n” must satisfy

$$n > 2 \quad (1)$$

Alternatively, the transformer primary winding current i_{Lr} will take a long time to decay to zero if “n” is too high. So “n” must be a moderate number. The equivalent inductance of the transformer is $L_r = L_{l1} + L_{l2}/n^2$ and is inversely proportional to the rise rate of the switching current when the auxiliary switch is turned on. It means that the equivalent inductance L_r should be high enough to limit the rising rate of the switch current to work in ZCS condition. The selection of L_r is determined using the following equation [14]

$$L_r \approx \frac{4t_{on}V_s}{I_{o\max}} \quad (2)$$

where t_{on} is the turn on time of an IGBT, and $I_{o\max}$ is the maximum load current. The snubber capacitance C_r is inversely proportional to the rise rate of the switching voltage drop when lower main inverter switches are turned off. This requires that the capacitance should be as high as possible to limit the rising rate of the voltage to work in ZVS condition. The selection of the snubber capacitor is determined using the following equation

$$C_r \approx \frac{4t_{off}I_{o\max}}{V_s} \quad (3)$$

where t_{off} is the turn off time of the IGBT. However, as the value of the capacitance increases, more energy is stored in it. This energy should be discharged when the main inverter switches are turned on. With high capacitance, the peak value of the transformer current will also be high. The peak value of i_{Lr} should be restricted to twice that of the maximum load current. From [12], we obtain

$$\sqrt{\frac{C_r}{L_r}} \leq \frac{nI_{o\max}}{(n-1)V_s} \quad (4)$$

Three lower switches of the inverter are turned on during mode-3. In order to turn on these switches at a fixed time the trailing edge of PWM for various load currents the following condition should be satisfied.

$$\frac{(\Delta t_1 + \Delta t_2 + \Delta t_3)}{I_o} = 0 > \frac{(\Delta t_1 + \Delta t_2)}{I_o} = I_{o\max} + t_{off} \quad (5)$$

The whole switching transition time is expressed as

$$\left. \begin{aligned} T_\omega &= \Delta t_1 + \Delta t_2 + \Delta t_3 + \Delta t_4 \\ &= \frac{nL_r I_o}{(n-1)V_s} + \sqrt{L_r C_r} \left[\cos \left(-\frac{1}{(n-1)} + \sqrt{n(n-2)} \right) \right] \end{aligned} \right\} \quad (6)$$

For high switching frequencies, T_ω should be as short as possible. The equivalent inductance (L_r) and snubber capacitance (C_r) are chosen to satisfy (1)–(5). L_r and C_r should be as small as possible. As the transformer operates at high frequency (20kHz), the magnetic core material can be ferrite. The design of the transformer needs the parameters such as form factor, frequency, the input/output voltage, input/output maximum current, and ambient temperature. From Fig. 2, the transformer current waveform can be simplified as triangular. The form factor is determined as $2/(3)^{1/2}$. Ambient temperature is dependent on the application field. Other parameters can be obtained from the previous section. Since the transformer carries current during the transition of turning on a switch in one cycle, the winding diameter can be smaller.

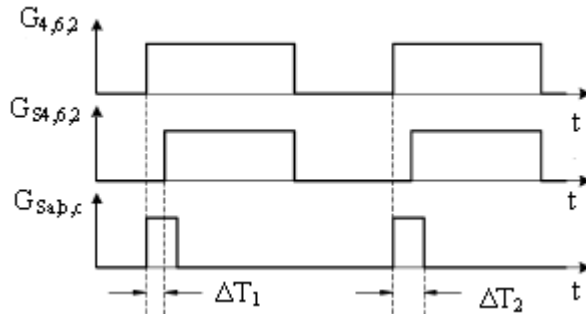


Figure 6: Gate signals $G_{S4,6,2}$ and $G_{Sa,b,c}$ from $G_{4,6,2}$.

Main switches S_1 to S_6 work under ZVS condition and therefore the voltage stress is equal to the dc link voltage V_s . The device current rate can be load current. Auxiliary switches S_a , S_b and S_c work under the ZVS (or) ZCS condition, while the voltage stress is also equal to the dc link voltage V_s . The peak current flowing through them is limited to double the maximum load current. As the auxiliary switches S_a , S_b and S_c carry the peak current only during switching transition, they can be rated with a lower continuous current rating. The additional cost will not be too much. The gate signals of three lower main inverter switches and auxiliary switches can be deduced from the output $G_{4,6,2}$ as shown in Fig. 6. The trailing edge of the gate signals for three lower main switches $G_{S4,6,2}$ is same as that of $G_{4,6,2}$, the leading edge of $G_{S4,6,2}$ lags behind $G_{4,6,2}$ for a short time ΔT_1 . The gate signals for auxiliary switches $G_{Sa,b,c}$ have a fixed pulse width (ΔT_2) with the leading edge, the same as that of $G_{4,6,2}$.

Controller Design

The transient response or dynamic behavior of any system depends on the controller being employed. In general, a conventional PI controller is used for most drive applications. But the conventional PI controller is slow and its tuning is a very serious problem if the system is complex to model mathematically. Further, if the system is non-linear then PI controller cannot work effectively. This leads to the search for other suitable controllers. One of the possible options for power electronic applications is the use of a fuzzy controller. Fuzzy controller design or tuning doesn't need any mathematical model of the system but needs the expertise and experience on the system and its behavior. Fuzzy controller has a good transient behavior, thereby making the system response fast. Also, the transient overshoot in the system is almost eliminated. Fuzzy controller is among the most suitable choices for system with non-linear characteristics. Hence, in this work the fuzzy controller is used to control the speed of BLDC motor with good dynamic response.

Proportional Integral Controller Design

The model of PI speed controller is given by,

$$G(S) = K_p + \frac{K_i}{S} \quad (7)$$

where $G(S)$ is the controller transfer function which is torque to error ratio in s-domain, K_p is the proportional gain and K_i is the integral gain. The tuning of these parameters is done using Ziegler Nichols method using the phase and gain margin specifications. The specifications of the drive application are usually available in terms of percentage overshoot and settling time. The PI parameters are chosen so as to place the poles at appropriate locations to get the desired response. These parameters are obtained using Ziegler Nichols method which ensures stability. From the dynamic response obtained by simulation, the percentage overshoot M_p and settling time t_s which are the measures of transient behaviour are obtained. The closed loop transfer function of the system is given by

$$T(S) = \frac{(K_p S + K_i)/J}{S^2 + \left(\frac{B + K_p}{J}\right)S + \frac{K_i}{J}} \quad (8)$$

where $T(S)$ is the closed loop transfer function and K_p , K_i are the PI controller parameters, J is the moment of inertia and B is the coefficient of friction. Comparing the characteristic equation (8) of the transfer function with a standard 2nd order system characteristic equation we get

$$K_p = 2\xi\omega_n J - B \quad (9)$$

$$K_i = J\omega_n^2 \quad (10)$$

Fuzzy Logic Controller Design

Fuzzy logic controller is a rule-based controller. It consists of an input, processing and output stages. The input or fuzzification stage maps sensor or other inputs such as switches, thumbwheels and so on, to the appropriate membership functions and truth values. The processing stage invokes each appropriate rule and generates a result for each, then combines the results of the rules. Finally, the output or defuzzification stage converts the combined result back into a specific control output. The membership function is triangular, although trapezoidal and bell curves are also used, but the shape is generally less important than the number of curves and their placement. From three to seven curves are generally appropriate to cover the required range of an input value or the “universe of discourse” in fuzzy language. There are several different ways to define the result of a rule, but one of the most common and simplest is the “max – min” inference method, in which the output membership function is given by the truth value generated by the premise. The simulation diagram of fuzzy logic controller is shown in Fig. 7.

Fuzzy rule has a 7×7 decision table with two input variables and one output variable. The look up table for the input and output rules defined for seven linguistic variables (NB, NM, NS, ZE, PS, PM, PB) that stand for negative big, negative medium, negative small, zero, controller converges to the reference value, positive small, positive medium and positive big respectively are given in Table. 1.

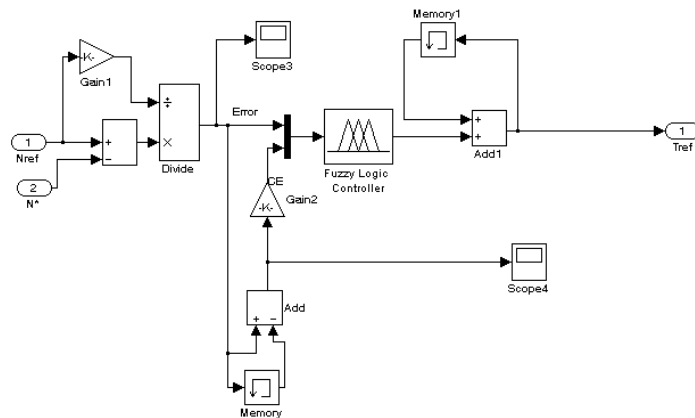


Figure 7: Simulation diagram of fuzzy logic controller.

For simplicity, membership function is expressed in exponential form as

$$\mu_{(x)} = \exp\left[1 - (x - a)^2 / 2b^2\right] \quad (11)$$

The membership function of intersection of any two inputs such as error (e) and change of error (Δe) is written as

$$\mu(i, j) = \min[\mu_e(i), \mu_{\Delta e}(j)] \quad (12)$$

where a, b are defined as an interval of each linguistic variable, x is the fuzzy input or output variables and i, j represent the number of labels 1, ..., 6, 7.

The triangular shaped membership functions are chosen due to their best control performance and simplicity. The height of the membership functions in this case is one. An overlap of 50% is provided for neighboring fuzzy subsets. Therefore at any point of the universe of discourse, no more than two fuzzy subsets will have non-zero degree of membership as shown in Fig. 8.

The inputs to the reference current generator are reference torque (T^*) and the rotor position signal (θ_r). The magnitude of the 3Φ current (I^*) is determined by using reference torque (T^*). Depending on the rotor position, the reference current generator generates the reference current (i_a^*, i_b^*, i_c^*). These reference currents are fed to the current controller.

Table 1: The Fuzzy Linguistic Rule Table.

$\Delta e \setminus e$	NB	NM	NS	Z	PS	PM	PB
NB	NB	NB	NB	NM	NS	NS	Z
NM	NB	NM	NM	NM	NS	Z	PS
NS	NB	NM	NS	NS	Z	PS	PM
Z	NB	NM	NS	Z	PS	PM	PB
PS	NM	NS	Z	PS	PS	PM	PB
PM	NS	Z	PS	PM	PM	PM	PB
PB	Z	PS	PS	PM	PM	PB	PB

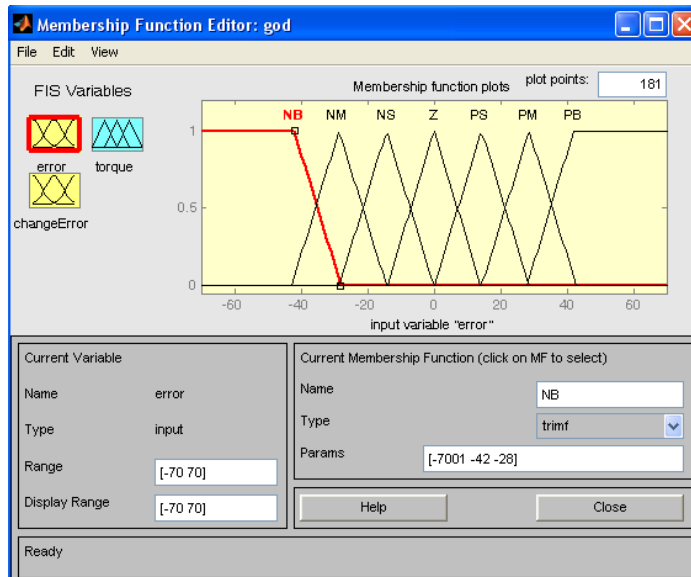
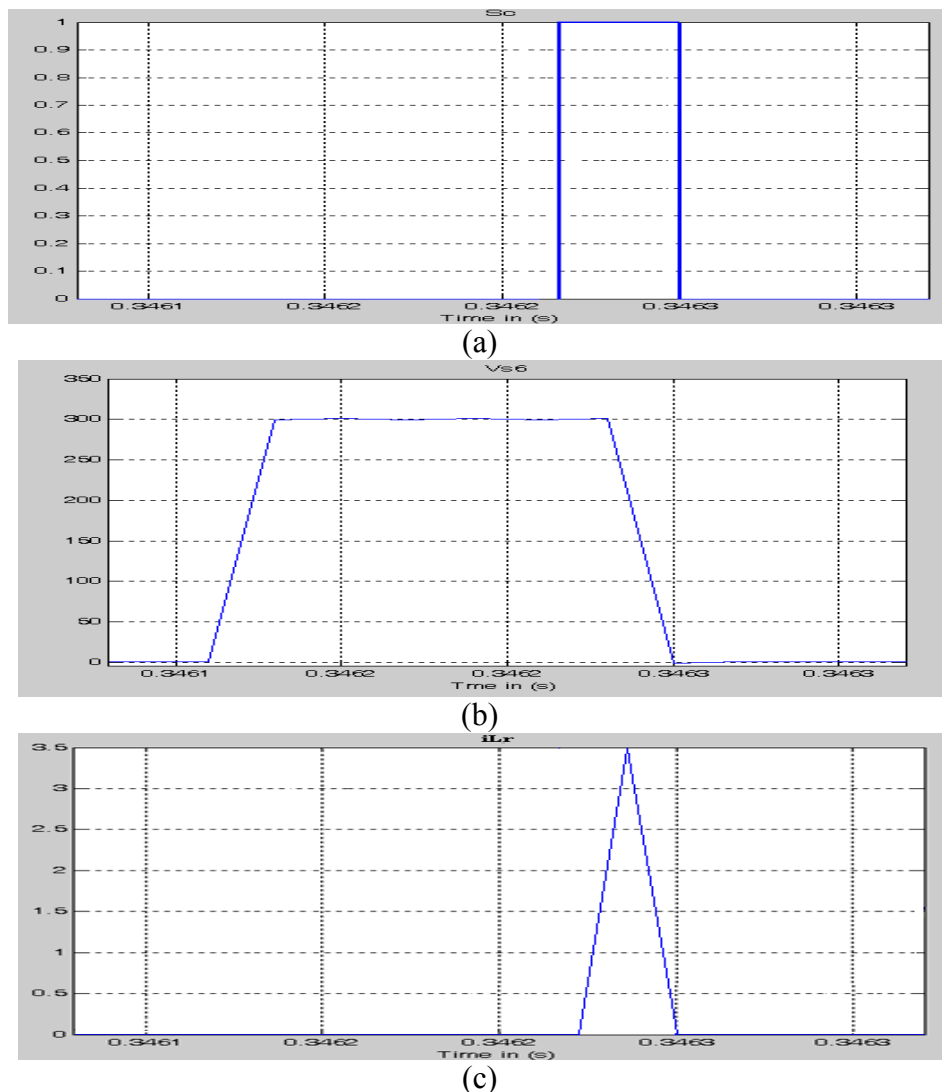


Figure 8: Membership function.

Simulation Results

The proposed inverter topology is verified by simulation software MATLAB 7.5. The dc link voltage V_S is chosen as 300 V. The parameters of the resonant circuit are determined from (1)–(6). The transformer turns ratio is chosen as 1 : 4 and the leakage inductance of the primary and secondary winding are 6 μH and 24 μH respectively. Therefore, the equivalent transformer inductance L_T is 7.5 μH . The resonant capacitance C_r is 0.047 μF . Then, $\Delta t_1 + \Delta t_2$ and $\Delta t_1 + \Delta t_2 + \Delta t_3$ can be determined for various load current I_o . The frequency of the PWM is 20 kHz. Waveforms of auxiliary switch gate signal (S_b), voltage drop across switch S_6 (u_{S6}), transformer primary winding current (i_{Lr}) and main switch gate signal (S_6) are shown in Fig. 9.

A BLDC motor with specifications as taken from [15] is shown in Table 2 and is simulated using MATLAB/ SIMULINK. The transient response of the motor for both PI and fuzzy controller are presented. The simulation was run for 1 seconds (simulation time).



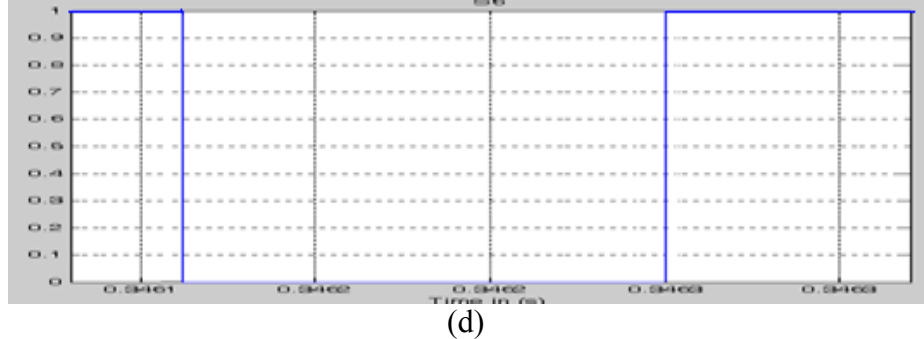


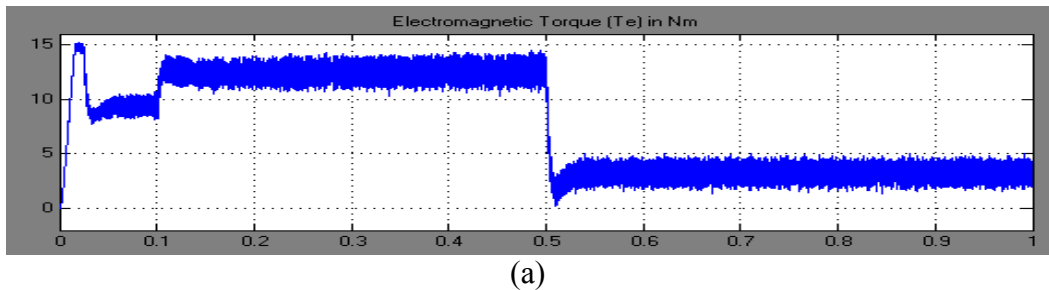
Figure 9: Simulation waveforms of (a) S_b (b) u_{s6} (c) i_{Lr} (d) S_6

Table 2: The Parameters of BLDC Motor.

Parameters		Value
DC Link Voltage	V_{dc}	300 V
Base Speed	ω_b	1000 rpm
Armature Resistance	R_a	2.875 Ω
Armature Inductance	L_a	8.5 mH
Magnetic Flux Linkage	Φ	0.175 wb
No. of Poles	P	4
Moment of Inertia	J	m^2
Friction Coefficient	B	0.005 Nm.s

Simulation Results with PI Controller

Substituting the values of the motor parameters and using Ziegler Nichols method, the tuning parameters are determined as $K_p=3.3$ and $K_i=300$. From Fig. 10(b) we obtain 0.4% overshoot and 0.53 seconds settling time. Fig. 10 shows electromagnetic torque for the reference speed of 500 rpm. Load torque is applied at 0.1 seconds.



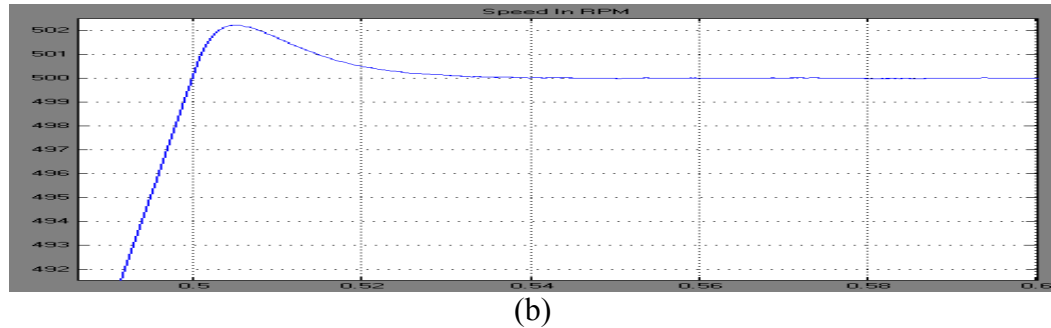
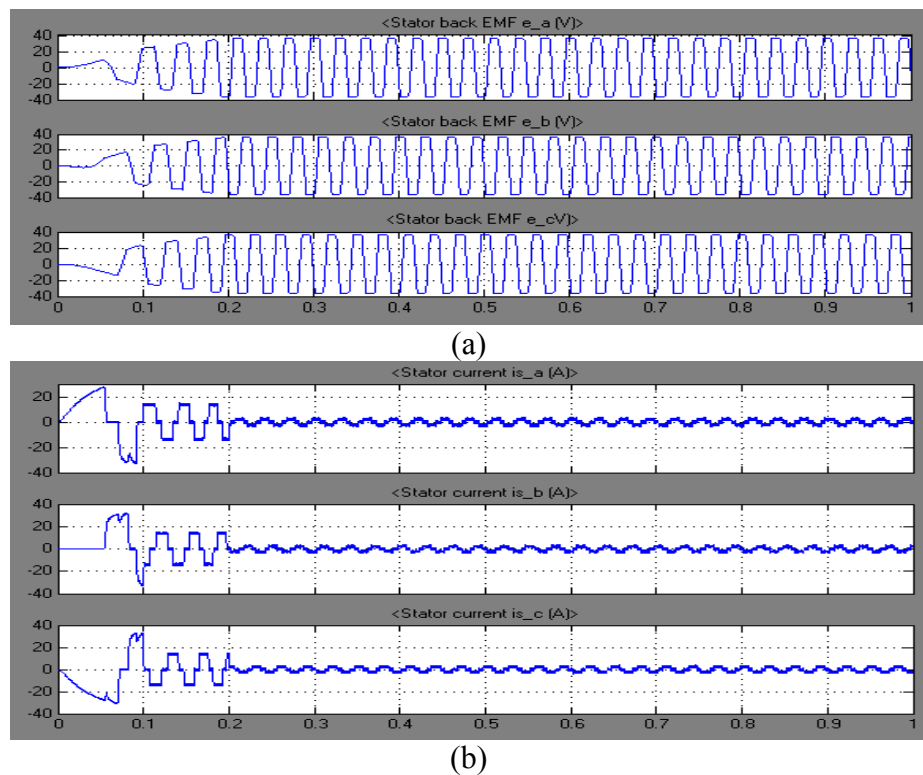


Figure 10: (a) Electromagnetic torque and (b) Speed response at 500 rpm with PI controller.

Simulation Results with Fuzzy Controller

Fig. 11 shows 3Φ back emfs, 3Φ currents and Electromagnetic torque for the reference speed of 500 rpm. Load torque is applied at 0.1 seconds. The 3Φ trapezoidal back emf and currents are almost with 120° phase difference. The speed response shows that the settling time of the motor with fuzzy controller is about 0.2 seconds and overshoot is almost eliminated with fuzzy controller. The speed of the PMBLDC motor, when controlled with the fuzzy controller shows better transient behavior of the drive system than the conventional PI controller.



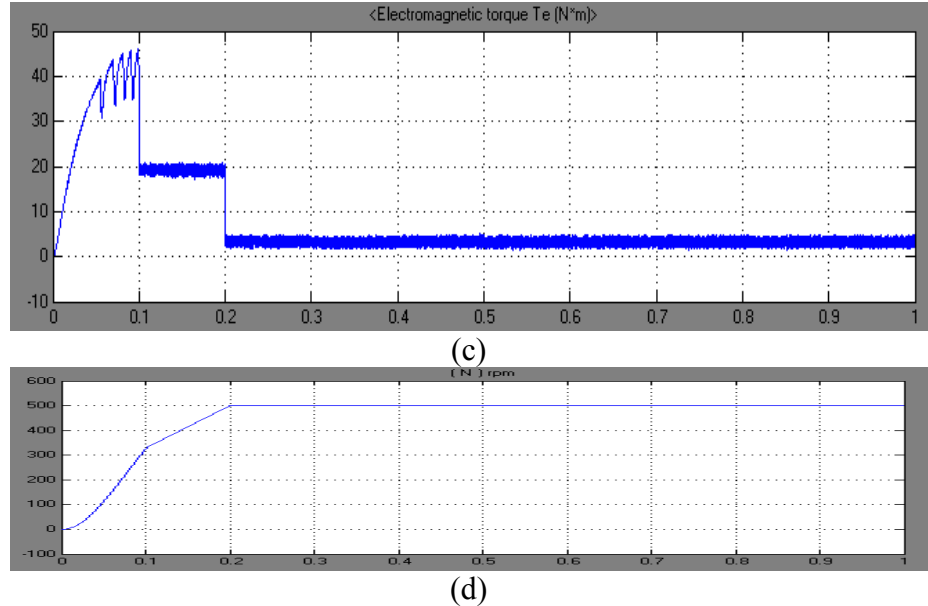


Figure 11: (a) 3Φ back emfs (b) 3Φ currents (c) Electromagnetic torque and (d) Speed response at 500 rpm with fuzzy controller

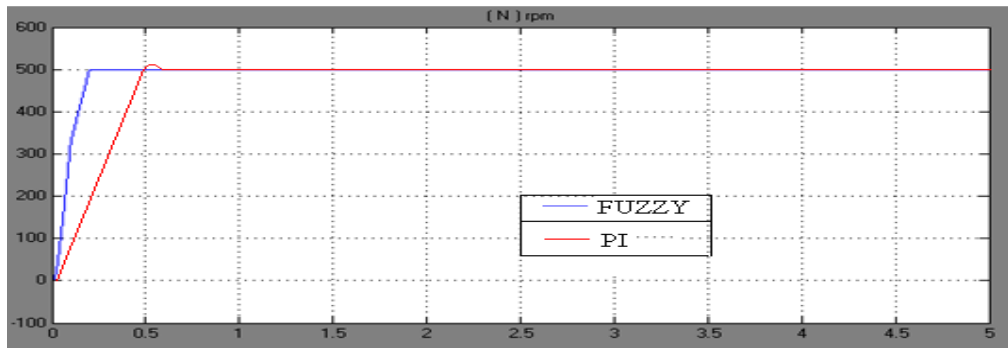


Figure 12: FLC Vs PI speed response for PMBLDC motor.

Table 3: Performance Analysis of Fuzzy and PI Controller.

Controller	Settling Time (Sec)	% Overshoot
FUZZY	0.2	0
PI	0.53	0.4

Fig. 12 shows the speed response of a PMBLDC motor for both fuzzy logic and PI controller and Table. 3 shows the dynamic performance specifications of fuzzy and PI controller. From the results obtained, it can be seen that the Soft switching inverter

works well under various load currents. Due to soft switching condition, the switching power losses is low. The efficiency Vs torque curves of hard switching and soft switching under rated speed are shown in Fig. 13, and it is observed that efficiency is improved with the soft switching inverter. This validates the Soft switching inverter topology used in this paper.

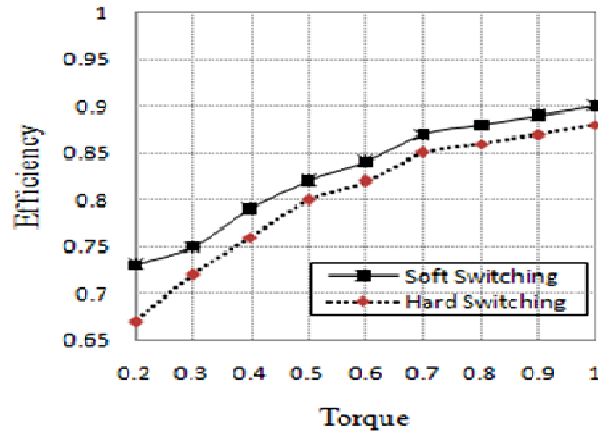


Figure 13: Efficiency Vs torque curves.

Conclusion

The performance analysis of a specially designed soft switching inverter for brushless dc motor drive system with two types of speed controllers namely PI and fuzzy based controller is presented. The dynamic behavior of the drive system with both controllers are presented and compared for a speed operation. It is observed that the fuzzy logic controller gives much better dynamic response for the system and is robust. From the results of proposed inverter topology, it can be seen that all the switches work under soft switching condition, freewheeling diodes are turned off under zero current condition which greatly reduces the reverse recovery problem of the diodes, voltage stress on all the switches is very low and it is not greater than the dc supply voltage, dv/dt and di/dt are reduced significantly hence EMI is reduced, very simple auxiliary switches control scheme is needed and the normal operation of the inverter is entirely the same as that of the hard switching inverter.

References

- [1] Dehmlow, M., Heumann, K., and Sommer, R., 1992, "Resonant Inverter Systems for Drive Applications", *EPE J.*, 2(4), pp. 225–232.
- [2] Divan, D. M., 1989, "The Resonant DC Link Converter - A New Concept in Static Power Conversion", *IEEE Transaction Industrial Application*, 25(2), pp. 317–325.

- [3] Divan, D. M., and Skibinski, G., 1989, "Zero – Switching Loss Inverters for High Power Applications", IEEE Transaction Industrial Application, 25(4), pp. 634–643.
- [4] Malesani, L., Tenti, P., Tomasin, P., and et al, 1995, "High Efficiency Quasiresonant DC Link Three-Phase Power Inverter for Full-Range PWM", IEEE Transaction Industrial Application, 31(1), pp. 141–148.
- [5] Jung, Y. C., Liu, H. L., Cho, G. C., and et al, 1995, "Soft Switching Space Vector PWM Inverter using a New Quasiparallel Resonant DC Link", Proc., IEEE Power Electronics Specialists Conference, pp. 936–942.
- [6] De Doncker, R. W., and Lyons, J. P., 1990, "The Auxiliary Resonant Commutated Pole Converter ", Proc., IEEE Industry Applications Society Annual Meeting, pp. 1228–1235.
- [7] McMurray, W., 1989, "Resonant Snubbers with Auxiliary Switches", Proc. IEEE Industry Applications Society Annual Meeting, pp. 289–834.
- [8] Vlatkovic,V., Borojevic, D., Lee, F., and et al, 1993, "A New Zero-Voltage Transition, Three-Phase PWM Rectifier /Inverter Circuit", Proc. IEEE Power Electronics Specialists Conference, pp. 868–873.
- [9] Cuadros, C., Borojevic, D., Gataric, S., and et al, 1994, "Space Vector Modulated, Zero-Voltage Transition Three-Phase to DC Bidirectional Converter", Proc.IEEE Power Electronics Specialists Conference, pp. 16–23.
- [10] Lai, J. S., Young Sr., R.W., Ott Jr., G.W., and et al, 1995, "A Novel Resonant Snubber Based Soft-Switching Inverter", Proc. Applied Power Electronics Conference Expo, pp. 797–803.
- [11] Lai, J.S., Young Sr., R.W., Ott Jr., and et al, 1996, "A Delta-Configured Auxiliary Resonant Snubber Inverter", IEEE Transaction Industrial Application, 32(3), pp. 518–525.
- [12] Zhi Yang Pan, and Fang Lin Luo, 2005, "Novel Resonant Pole Inverter for Brushless DC Motor Drive System", IEEE Transactions on Power Electronics, 20(1), pp. 173 – 181.
- [13] Miller, T. J. E., 1989, Brushless Permanent-Magnet and Reluctance Motor Drives, Clarendon, Oxford, U.K.
- [14] Divan, D. M ., Venkataramanan, G., and De Doncker, R. W., 1987, "Design Methodologies for Soft Switched Inverters", Proc. IEEE Industry Applications Society Annual Meeting, pp. 626–639.
- [15] Hai Lin, Weisheng Yan, Jinhua Wang, and et al, 2009, "Robust Nonlinear Speed Control for a Brushless DC Motor Using Model Reference Adaptive Backstepping Approach", Proc. IEEE Industry Applications Conference, pp. 335-340.